

# Analysis of Residence Time in the Measurement of Radon Activity by Passive Diffusion in an Open Volume: A Micro-Statistical Approach

M. P. Silverman

Department of Physics, Trinity College, Hartford, CT, USA  
Email: mark.silverman@trincoll.edu

**How to cite this paper:** Silverman, M.P. (2017) Analysis of Residence Time in the Measurement of Radon Activity by Passive Diffusion in an Open Volume: A Micro-Statistical Approach. *World Journal of Nuclear Science and Technology*, 7, 252-273. <https://doi.org/10.4236/wjnst.2017.74020>

**Received:** July 12, 2017

**Accepted:** August 27, 2017

**Published:** August 30, 2017

Copyright © 2017 by author and Scientific Research Publishing Inc. This work is licensed under the Creative Commons Attribution International License (CC BY 4.0). <http://creativecommons.org/licenses/by/4.0/>



Open Access

## Abstract

Residence time in a flow measurement of radioactivity is the time spent by a pre-determined quantity of radioactive sample in the flow cell. In a recent report of the measurement of indoor radon by passive diffusion in an open volume (*i.e.* no flow cell or control volume), the concept of residence time was generalized to apply to measurement conditions with random, rather than directed, flow. The generalization, leading to a quantity  $\Delta t_r$ , involved use of a) a phenomenological alpha-particle range function to calculate the effective detection volume, and b) a phenomenological description of diffusion by Fick's law to determine the effective flow velocity. This paper examines the residence time in passive diffusion from the *micro-statistical* perspective of single-particle continuous Brownian motion. The statistical quantity "mean residence time"  $T_r$  is derived from the Green's function for unbiased single-particle diffusion and is shown to be consistent with  $\Delta t_r$ . The finite statistical lifetime of the randomly moving radioactive atom plays an essential part. For stable particles,  $T_r$  is of infinite duration, whereas for an unstable particle (such as  $^{222}\text{Rn}$ ), with diffusivity  $D$  and decay rate  $\lambda$ ,  $T_r$  is approximately the effective size of the detection region divided by the characteristic diffusion velocity  $\sqrt{D\lambda}$ . Comparison of the mean residence time with the time of first passage (or exit time) in the theory of stochastic processes shows the conditions under which the two measures of time are equivalent and helps elucidate the connection between the phenomenological and statistical descriptions of radon diffusion.

## Keywords

Radon, Diffusion, Brownian Motion, Random Walk, Residence Time,

## 1. Introduction: Residence Time in the Measurement of Radon Activity

### 1.1. Measurement of Radon by Geiger-Mueller Detectors

Of the many sources and causes of airborne radioactive contamination [1], the naturally occurring contaminant radon is perhaps the most pervasive, since it arises as one of the daughter products, and the only radioactive gas, in the decay series of uranium-238 ( $^{238}\text{U}$ ), uranium-235 ( $^{235}\text{U}$ ), and thorium-232 ( $^{232}\text{Th}$ ) dispersed widely in rocks and soils throughout the Earth. The radon isotope with the longest half-life,  $^{222}\text{Rn}$ , is of particular concern. The World Health Organization (WHO) reports  $^{222}\text{Rn}$  to be the leading cause of lung cancer among people who have never smoked, and to significantly increase the risk of lung cancer over that due to smoking alone in those who do smoke or have smoked in the past [2]. Although no level of indoor radon exposure is regarded as safe, the WHO recommends a reference level of  $100 \text{ Bq/m}^3$  to minimize health hazards (Ref [2], p. ix). Similarly, the US Environmental Protection Agency (EPA) recommends a level of  $4 \text{ pCi/L}$  above which remedial action should be taken [3]. (For comparison, note that  $1 \text{ picocurie per liter} = 37 \text{ becquerel per cubic meter}$ .) It is desirable, therefore, in view of the health risks posed by radon, to develop methods to measure indoor radon activity in a rapid, accurate, convenient, and inexpensive way.

In a recent paper [4] Silverman proposed and demonstrated the use of two pancake-style Geiger-Mueller (GM) counters to measure quantitatively the activity concentration, *i.e.* activity per unit volume, of radon-222 ( $^{222}\text{Rn}$ ) by passive diffusion *without* the requirement, common to virtually all other methods of radon measurement, of a fixed instrumental control volume. This new measurement protocol enables the user to determine radon concentration immediately after a short-term (e.g. 24 hour) sampling time, thereby eliminating the cost, delay, and sample loss of sending samples to an external testing laboratory for analysis. Application of the GM method yielded results of equivalent accuracy and higher precision, particularly in repeated short-term measurements, in comparison with results obtained concurrently with state-of-the-art certified commercial radon detectors also utilizing passive diffusion.

Briefly summarized, the reported GM method employed one GM detector to record counts of  $\alpha$ ,  $\beta$ , and  $\gamma$  particles, and the other GM detector, covered with an alpha-blocking layer, to record just  $\beta$ , and  $\gamma$  particles. The detectors were located so that the count-rate difference was exclusively attributable to alpha detection from  $^{222}\text{Rn}$  and its polonium progeny  $^{218}\text{Po}$ ,  $^{214}\text{Po}$  in the room air—*i.e.* not contaminated by emissions from radioactive elements in the construction materials of surrounding surfaces. Theoretical analysis based on the

physics of atomic diffusion in air and alpha particle interactions in matter provided the means to convert the alpha count rate (e.g. cpm = counts per minute) into a radon activity concentration (Bq/m<sup>3</sup> or pCi/L).

The methodology and accompanying analysis in [4] relied on the short range of alpha transmissivity in matter. For example, the 5.49 MeV alpha emitted in the decay of <sup>222</sup>Rn to <sup>218</sup>Po is about 4 cm in air (at 1 atm and 20°C). Moreover, the energy loss of an alpha particle per collisional interaction is approximately a constant 35 eV for each ionizing encounter [5], leading to a transmission probability that is essentially constant over the greater part of the particle's range, then decreasing rapidly to zero after a total of about  $1.5 \times 10^5$  interactions. It is this feature that enabled [4] to represent the alpha transmission through air (or a condensed medium like the thin mica window of the GM detector) by a phenomenological range function of the form

$$Q_\kappa(r) = \left[ \exp \left\{ \kappa \left( \frac{r}{R_\alpha} - 1 \right) \right\} + 1 \right]^{-1} \quad (1)$$

whose variation with distance  $r$  from the alpha point of origin is shown in the solid red plot of **Figure 1** for the 5.49 MeV alpha in air. The red trace calculated from Equation (1) with alpha range parameter  $R_\alpha = 4.03$  cm and fall-off parameter  $\kappa = 28$  is visually indistinguishable from the empirical alpha transmissivity curve [6]. The mean range  $R_\alpha$ , marked by the dashed black vertical line is defined by the distance at which alpha transmission is 50%, as indicated by the dashed black horizontal line in the figure. The fluctuation in alpha range values about  $R_\alpha$  as the particle rapidly comes to rest is closely represented by a Gaussian distribution  $N(R_\alpha, \sigma^2)$  (dashed blue curve) with relative uncertainty  $\sigma/R_\alpha$  of ~5% [7]. In the figure, the amplitude of the Gaussian is scaled down by a factor 2 to facilitate visual presentation of both plots.

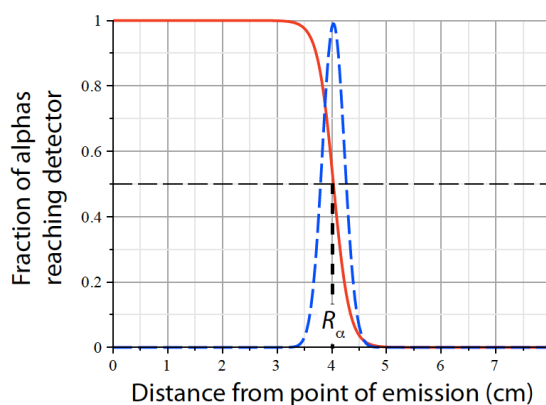


**Figure 1.** Plot of 5.49 MeV alpha transmissivity in air (solid red) as modeled by range function  $Q_\kappa(r)$  for mean range  $R_\alpha = 4.03$  cm and fall-off parameter  $\kappa = 28$ . Superposed is the Gaussian distribution  $N(R_\alpha, \sigma_R^2)$  (dashed blue) of range variations about  $R_\alpha$  with  $\sigma_R/R_\alpha = 0.05$ . The horizontal dashed line marks 50% transmission; the vertical dashed line locates  $R_\alpha$ .

## 1.2. Radon Transport as a Process of Macroscopic Diffusion

The measurement procedure described in [4] pertained primarily to the diffusive ingress of radon through a single external subterranean (or partly subterranean) wall, such as commonly occurs in the basements of residences and research labs. For purposes of mathematical modeling, these conditions entail one-dimensional atomic diffusion from a planar source. For atoms diffusing from the source at the wall through the room air and over the GM detectors, positioned so that the detector windows are horizontal (in the plane  $z = 0$ ) and facing upward, the effective detection volume  $V_d$  in the half space  $z \geq 0$  (centered on each detector window) and effective cross section  $A_d$  of flow through a surface  $\Sigma$  normal to the GM window were defined and evaluated in [4] by means of  $Q_\kappa(r)$  as follows

$$V_d = \iiint_{z>0} Q_\kappa(r) dV = 2\pi \int_0^\infty r^2 Q_\kappa(r) dr \quad (2)$$

$$A_d = \iint_{\Sigma} Q_\kappa(r) d\Sigma = 2\pi \int_0^\infty r Q_\kappa(r) dr. \quad (3)$$

Although the integrations are theoretically over the volume and cross section of the entire room (or, as a practical matter, over an infinite range for a room size  $\gg R_\alpha$ ) rather than over the finite space and surface of an instrumental control volume, the constraint posed by the alpha range function  $Q_\kappa(r)$  leads to finite results. For example, evaluation of Equations (2) and (3) for the 5.49 MeV alpha of  $^{222}\text{Rn}$  in air yielded  $V_d(^{222}\text{Rn}) = 138.8 \text{ cm}^3$  and  $A_d(^{222}\text{Rn}) = 51.2 \text{ cm}^2$ .

For measurements of radioactivity executed over a period of time in an open volume, it is necessary to determine the rate at which radioactive atoms pass through the region of detectability. This was accomplished in [4] by modeling the detection process as a radioactive flow measurement [8], such as employed in high-performance radioactive liquid chromatography [9], by defining an effective residence time  $\Delta t_r$ ,

$$\Delta t_r = V_d / v_0 A_d \quad (4)$$

in which

$$v_0 = \sqrt{D_0 \lambda_0} = (4.81 \pm 0.22) \times 10^{-6} \text{ m/s} \quad (5)$$

is the flow velocity determined by the  $^{222}\text{Rn}$  diffusion coefficient [10] [11]

$$D_0 = (1.1 \pm 0.1) \times 10^{-5} \text{ m}^2 \cdot \text{s}^{-1} \quad (6)$$

and decay rate [12]

$$\lambda_0 = (2.098 \pm 0.0004) \times 10^{-6} \text{ s}^{-1}. \quad (7)$$

In a conventional flow measurement, the sample consists of a stream that passes through a flow cell aligned perpendicular to the detector surfaces. The detectors, which are photomultiplier tubes in the case of flow scintillation counting, therefore sample the radioactive material only for the time that the

atoms reside in the flow cell. This residence time is the ratio of the flow velocity and sample flow rate (in units of volume per time). In liquid chromatography the flow velocity is a well-defined, experimentally adjustable quantity, but in the diffusion of a radioactive gas it is a characteristic parameter of a stochastic process. Expression (5) was derived in [4] by solution of the one-dimensional steady-state diffusion equation with implementation of open-volume boundary conditions and account taken of loss by radioactive decay.

Although not reported in [4], the integrals in Equations (2) and (3) upon substitution of range function (1) can be expressed in terms of known special functions yielding the following closed forms for the effective detection volume and area

$$V_d = \frac{2}{3} \pi R_\alpha^3 \left[ 1 + \left( \frac{\pi}{\kappa} \right)^2 - \frac{6 \text{Li}_3(-e^{-\kappa})}{\kappa^3} \right] \quad (8)$$

$$A_d = \pi R_\alpha^2 \left[ 1 + \frac{1}{3} \left( \frac{\pi}{\kappa} \right)^2 + \frac{2 \text{Li}_2(-e^{-\kappa})}{\kappa^2} \right] \quad (9)$$

in which

$$\text{Li}_s(z) = \sum_{n=1}^{\infty} \frac{z^n}{n^s} \quad (10)$$

is the polylogarithm function. For index  $s = 2$ , the function is related to the dilogarithm function

$$\text{dilog}(x) \equiv \int_1^x \frac{\ln y}{1-y} dy = \text{Li}_2(1-x). \quad (11)$$

Use of the preceding expressions (8) and (9) together with relations (4) and (5) leads to the following closed form expression for the residence time

$$\Delta t_r = \frac{2R_\alpha}{3\sqrt{D\lambda}} \left( \frac{1 + (\pi/\kappa)^2 - (6/\kappa^3) \text{Li}_3(-e^{-\kappa})}{1 + \frac{1}{3}(\pi/\kappa)^2 + (2/\kappa^2) \text{Li}_2(-e^{-\kappa})} \right). \quad (12)$$

Evaluation of relation (12) for passive diffusion of  $^{222}\text{Rn}$  in air yields a residence time  $\Delta t_r = 5637 \text{ s} \sim 1.57 \text{ h}$ .

Although residence time defined in terms of the diffusive flow of a macroscopic current of radioactive gas resulted in values of radon concentration in accord with measurements by a calibrated standard, it is nevertheless of interest, both conceptually and practically, to examine the concept of residence time from a micro-statistical perspective of particle Brownian motion. For one, this latter approach avoids the adoption of a phenomenological range function with adjustable parameter  $\kappa$ . And for another, the examination of radon transport by Brownian motion sheds light on the physical process of diffusion, clarifies theoretical points concerning the calculation of expectation values, and distinguishes the statistical concept of residence time from the concept of time of first passage,

which frequently arises in the study of stochastic processes. These two approaches—macro-statistical diffusion and micro-statistical Brownian motion—address two differently expressed, but basically equivalent, practical questions. In the former (diffusion), the question is “On average how many particles per unit time flow through the detection region?”; in the latter (Brownian motion), the question is “On average how long does one particle remain in the detection region?”.

The development and investigation of such a micro-statistical model is the principal objective of this paper. This is accomplished in the following sections by calculating the exact time-dependent probability density (Green’s function) for Brownian motion of radon from a planar source and showing that a certain integral of this function over time provides the sought-for statistical expectation value corresponding to the residence time in the macro-statistical model developed in [4]. In this regard, Equations (8), (9), and (12) will be useful later in the comparison of the residence time as modeled in [4] with the mean residence time obtained from the micro-statistical treatment developed in this paper.

## 2. Micro-Statistical Calculation of Residence Time

### 2.1. Conditional Probability for Single-Particle Brownian Motion with Decay

The equation for the conditional probability  $G(\mathbf{r}, t | \mathbf{r}', 0)$  of diffusion of an unstable particle from some source point  $\mathbf{r}' = (x', y', z')$  at time  $t' = 0$  to a field point  $\mathbf{r} = (x, y, z)$  at time  $t$  with diffusion coefficient  $D$  and decay rate  $\lambda$  takes the form [13] [14]

$$\frac{\partial G(\mathbf{r}, t | \mathbf{r}', 0)}{\partial t} - D\nabla^2 G(\mathbf{r}, t | \mathbf{r}', 0) = -\lambda G(\mathbf{r}, t | \mathbf{r}', 0) \quad (13)$$

and leads to the solution

$$G(\mathbf{r}, t | \mathbf{r}', 0) = \frac{1}{(4\pi Dt)^{3/2}} \exp\left(-\frac{|\mathbf{r} - \mathbf{r}'|^2}{4Dt}\right) e^{-\lambda t}. \quad (14)$$

The Green’s function expressed in Equation (14) is a three-dimensional Gaussian conditional probability density—*i.e.* a probability per unit volume—as indicated by the dimensionality  $[(Dt)^{-3/2}] = [\text{Length}^{-3}]$  of the right side of the equation.

In a coordinate system with vertical  $z$ -axis and horizontal  $x$ -axis directed normally outward from the particle source plane ( $x' = 0$ ), the probability density for arrival of a particle at  $\mathbf{r}$  irrespective of the initial location  $(0, y', z')$  of the particle in the source plane is obtained by integrating (14) over the coordinates  $y', z'$  as follows:

$$p(x, t) = (4\pi Dt)^{-3/2} e^{-\lambda t} \int_{-\infty}^{\infty} \int_{-\infty}^{\infty} e^{-|r-r'|^2/4Dt} f(x', y') dx' dy' = (4\pi Dt)^{-1/2} e^{-x^2/4Dt} e^{-\lambda t} \quad (15)$$

where  $f(x', y')$  is the prior probability (in a Bayesian sense), assumed to be

uniform, of the particle distribution in the source plane. Since  $f(x', y')$  is a constant, it can be assigned whatever numerical value makes  $p(x, t)$  a function whose integral over the entire  $x$ -axis is unity. Taking  $f(x', y') = 1$  leads to the second equality in (15), which is equivalent to the Green's function for one-dimensional diffusion with decay from a delta function source.

The function  $p(x, t)$  in Equation (15), plotted in **Figure 2**, is the conditional probability density for finding a particle within the vertical plane located at horizontal coordinate  $x$  at time  $t$ , given that the particle was in the plane  $x = 0$  at  $t = 0$ . To keep symbolic notation as simple as possible where there is no confusion, the initial (0,0) condition is not explicitly shown in the argument. Nevertheless, it bears emphasizing that the coordinates expressed in Equation (15) are actually spatial and temporal *intervals*. Moreover, radioactive decay is a Markov or “memoryless” process [15]—that is, an unstable nucleus does not age, but has the same probability of decay within a specified time interval irrespective of when the interval was begun. Therefore, Equation (15) applies whether the source plane is taken to be the wall through which radon enters the room or a plane (to be adopted shortly) bisecting the detection volume above the detector window.

Reduction of the problem of 3-dimensional diffusion from a planar source to diffusion from a point source on the horizontal axis is a consequence of the isotropic symmetry of Equation (14), which permits factorization into a product of three independent one-dimensional degrees of freedom. The isotropic symmetry itself comes from neglect of gravity, the effects of which are shown in **Appendix 1** to be negligible under the circumstances of measuring radon activity by the method developed in [4] and elaborated further in this paper.

From Equation (15), one can calculate the cumulative probability  $P(\ell \geq x \geq -\ell, t)$  of the particle being somewhere between the plane  $x = -\ell$  (entrance plane of the detection region) and  $x = \ell$  (exit plane of the detection

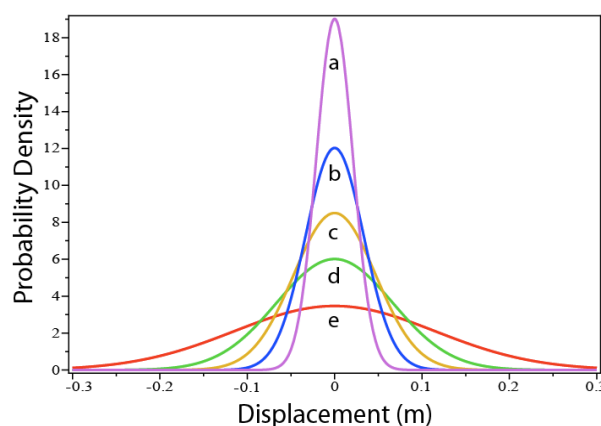


**Figure 2.** Probability density of one-dimensional unconstrained Brownian motion (Equation (15)) as a function of displacement starting at the origin for times (s): (a) 20 (violet); (b) 50 (blue); (c) 100 (gold); (d) 200 (green); (e) 600 (red). Radon parameters:

$$D_0 = 1.1 \times 10^{-5} \text{ m}^2 \cdot \text{s}^{-1}, \quad \lambda_0 = 2.1 \times 10^{-6} \text{ s}^{-1}.$$

region) during the time interval  $t$  begun when the particle was placed at  $x = 0$  (the vertical plane bisecting the detection region centered above the detector window)

$$P(\ell \geq x \geq -\ell, t) = \frac{e^{-\lambda t}}{\sqrt{4\pi Dt}} \int_{-\ell}^{\ell} e^{-x^2/4Dt} dx = \operatorname{erf}\left(\frac{\ell}{\sqrt{4Dt}}\right) e^{-\lambda t}. \quad (16)$$

The error function in Equation (16) is defined by

$$\operatorname{erf}(x) = \frac{2}{\sqrt{\pi}} \int_0^x e^{-u^2} du = -\operatorname{erf}(-x) \quad (17)$$

and is an anti-symmetric function of its argument.

The time interval  $T_r$  (mean statistical residence time) of a particle within the detection region is then obtained by averaging over all values of the interval  $t$  in Equation (16) by the following integral

$$T_r = \int_0^{\infty} P(\ell \geq x \geq -\ell, t) dt = \lambda^{-1} (1 - e^{-\ell/\zeta}) \quad (18)$$

in which

$$\zeta = \sqrt{D/\lambda} \quad (19)$$

is the characteristic diffusion length. (See Ref. [4], **Appendix 1**) For  $^{222}\text{Rn}$ , it follows from relations (6) and (7) that

$$\zeta_0 = \sqrt{D_0/\lambda_0} = 2.29 \pm 0.10 \text{ m}. \quad (20)$$

In the limit that  $\ell \rightarrow \infty$  in Equation (18), the residence time  $T_r \rightarrow \lambda^{-1}$ , the statistical lifetime of the unstable nucleus. (Note: the lifetime  $\lambda^{-1}$  and half-life  $\tau_{1/2}$  are related by  $\tau_{1/2} = \lambda^{-1} \ln 2$ .)

The mean value  $T_r$  expressed in Equation (18) calls for a brief explanation because its justification comes from a statistical relation that may not be widely familiar. Ordinarily, the expectation value  $\langle T \rangle$  of a distributed quantity (*i.e.* random variable)  $T$  is performed by an integration weighted by a probability density function (pdf)  $\phi(t)$  in an expression like

$$\langle T \rangle = \int_0^{\infty} t \phi(t) dt \quad (21)$$

in which  $\phi(t) dt$  is the probability that a realization  $t$  of random variable  $T$  falls within the interval  $(t, t + dt)$ . However,  $P(\ell \geq x \geq -\ell, t)$  in Equation (16) is *not* the probability density for residence time  $T$ . Moreover, it is dimensionless, so that to multiply  $P(\ell \geq x \geq -\ell, t)$  by  $t$  and integrate over a range of  $t$  would lead to a quantity that has the incorrect dimension of time squared.

A procedure entirely equivalent to (21) for computing expectation values is to use the cumulative distribution function (cdf)  $F(t)$  defined as the probability  $P(T \leq t)$  given by

$$F(t) = \int_{-\infty}^t \phi(s) ds. \quad (22)$$

It can then be shown (in **Appendix 2**) that the expectation value  $\langle T \rangle$  takes the form

$$\langle T \rangle = \int_0^\infty (1 - F(t)) dt - \int_{-\infty}^0 F(t) dt. \tag{23}$$

For a random variable defined on the positive real axis only, the second term on the right side of Equation (23) vanishes. This is the case for  $P(\ell \geq x \geq -\ell, t)$ , which can be related to the cdf of the residence time by the following argument. The probability  $P(\ell \geq x \geq -\ell, t)$  that the particle lies in a region between  $-\ell$  and  $\ell$  after time interval  $t$  means that the actual residence time  $T$  must be greater than  $t$ , otherwise the particle would have left the region. Thus, one can write the equivalence

$$P(\ell \geq x \geq -\ell, t) = P(T > t) = 1 - F(t) \tag{24}$$

where the second equality in Equation (24) follows from the definition (22) of the cumulative distribution function. Since  $F(t) = 0$  for  $t < 0$ , it then follows from relations (23) and (18) that

$$T_r \equiv \langle T \rangle = \int_0^\infty (1 - F(t)) dt = \int_0^\infty P(\ell \geq x \geq -\ell, t) dt. \tag{25}$$

### 2.2. Comparison of Phenomenological and Statistical Residence Time Functions

For purposes of comparison, the two expressions for residence time are collected below with substitution of the characteristic diffusion length (19)

$$\text{Phenomenological: } \Delta t_r = \frac{2R_\alpha}{3\sqrt{D\lambda}} \left( \frac{1 + (\pi/\kappa)^2 - (6/\kappa^3) \text{Li}_3(-e^{-\kappa})}{1 + \frac{1}{3}(\pi/\kappa)^2 + (2/\kappa^2) \text{Li}_2(-e^{-\kappa})} \right) \tag{26}$$

$$\text{Statistical: } T_r = \lambda^{-1} \left( 1 - \exp(-\ell\sqrt{\lambda/D}) \right). \tag{27}$$

Numerical evaluation of the statistical residence time (27) requires substitution of a specific length  $L = 2\ell$  of the detection volume  $V_d$ . Since a fixed length implies a sharply defined volume  $V_d$ , such a substitution corresponds to a phenomenological residence time (26) in the limit  $\kappa \rightarrow \infty$ , as illustrated by plot (f) in **Figure 3**. Moreover, since the characteristic diffusion length (20) for  $^{222}\text{Rn}$  is about 2.3 m and the range of the alpha particle in air is only about 0.04 m, the exponent in Equation (27) is  $\ell/\zeta \sim 0.017 \ll 1$ . It is therefore appropriate to compare

$$\lim_{\kappa \rightarrow \infty} \Delta t_r \rightarrow \frac{2}{3} \frac{R_\alpha}{\sqrt{D\lambda}} \tag{28}$$

with the Taylor series expansion of relation (27) truncated at the lowest order of  $\ell/\zeta$

$$\lim_{\zeta \rightarrow \infty} T_r \rightarrow \frac{\ell}{\lambda\sqrt{D/\lambda}} = \frac{\ell}{\sqrt{D\lambda}} = \frac{1}{2} \frac{L}{\sqrt{D\lambda}}. \tag{29}$$

For the two expressions (28) and (29) to yield the same residence time interval, the effective length of the detection volume  $L$  would be related to the mean alpha range by

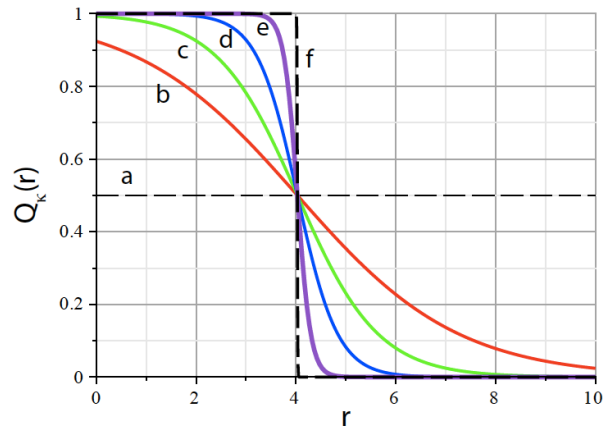


**Figure 3.** Plot of range function  $Q_\kappa(r)$  as function of  $r$  for parameter  $\kappa$  equal to (a) 0 (thin black dash); (b) 2.5 (red); (c) 5 (green); (d) 20 (blue); (e) 50 (violet), (f)  $\infty$  (thick black dash). For  $\kappa = \infty$ ,  $Q_\kappa(r)$  takes the form of a step function.

$$L = 4R_\alpha/3. \quad (30)$$

For the case of a 5.49 MeV alpha in air with experimental mean range  $R_\alpha = 4.03$  cm, relation (30) leads to a detection volume of horizontal length  $L = 5.37$  cm, which, as shown in **Figure 1**, corresponds very closely to the distance through air at which the alpha range function  $Q_\kappa(r)$  is perceived to drop to 0. Exact numerical evaluation of residence times (26) and (27) for  $L$  given by relation (30) yields

$$\begin{aligned} \Delta t_r &= 5636.7 \text{ s} = 1.57 \text{ h} \\ T_r &= 5524.8 \text{ s} = 1.54 \text{ h} \end{aligned} \quad (31)$$

which are in excellent accord.

From the definition (22) of the cdf, one obtains the corresponding pdf by application of the Leibniz rule [16] for differentiating an integral

$$p(t) = dF(t)/dt. \quad (32)$$

It then follows from relation (24) that the pdf for the random variable  $T$  whose expectation is the residence time  $T_r$  is given by

$$p_T(t) = \frac{d}{dt} \left( 1 - e^{-\lambda t} \operatorname{erf} \left( \frac{\ell}{\sqrt{4Dt}} \right) \right) = e^{-\lambda t} \left[ \frac{\ell \exp(-\ell^2/4Dt)}{\sqrt{4\pi Dt^3}} + \lambda \operatorname{erf} \left( \frac{\ell}{\sqrt{4Dt}} \right) \right]. \quad (33)$$

**Figure 4** shows a plot of pdf (33) as a function of time for parameters characteristic of  $^{222}\text{Rn}$  with  $\ell$  given by expressions (29) and (30). The sharp rise (to a maximum  $T_{\max} \approx 34$  s) with long “fat tail” of the pdf resembles an inverse Gaussian or Levy distribution. The first term ( $\propto t^{-3/2}$ ) on the right hand side of pdf (33), known as the Smirnov density [17], derives exclusively from continuous Brownian motion; the second term depends on radioactive decay and would be absent if the diffusing particle were stable ( $\lambda = 0$ ). It is to be noted that the mean residence time for a diffusing stable particle, whether calculated

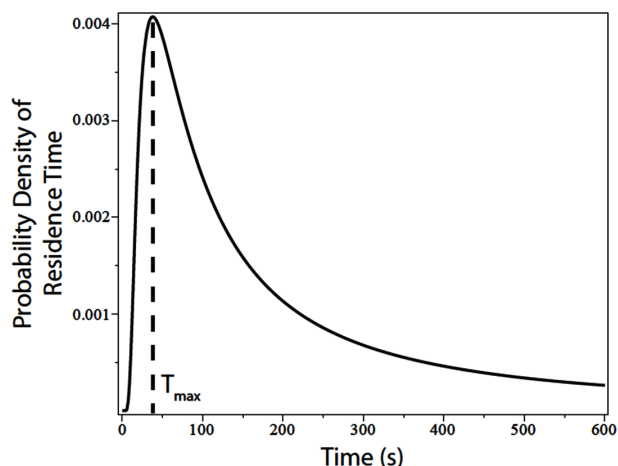


**Figure 4.** Probability density (Equation (33)) of the residence time of a particle in the region  $l \geq x \geq -l$ , plotted for the radon parameters of **Figure 2** and length  $l = 0.05$  m. The steep rise and long tail resemble an inverse Gaussian or Levy distribution. The maximum occurs at  $\sim 38$  s; the mean is  $\sim 5557$  s.

simply by relation (25) or much more onerously from expression (21) with  $\phi(t)$  replaced by pdf (33), is infinite. One sees this explicitly by taking the limit of Equation (27) as  $\lambda \rightarrow 0$ . The interpretation of this result for a stable particle undergoing one-dimensional Brownian motion, as is demonstrated in books on stochastic processes [18], is that the particle will eventually return to a specified location with a probability of 100%, but on average only after a random walk of infinite duration. However, an unstable particle, which does not survive long enough to take an infinite walk, has a finite mean residence time—a result that one would of course expect on physical grounds.

In the following section the residence time is obtained in a different way by examining stochastic events referred to as “first passage” or “first return”, which occur widely in problems involving Brownian motion with boundaries.

### 2.3. Comparison of Residence Time with First Passage Time to One Absorbing Boundary

The time of first passage (FPT) is the time for a particle undergoing Brownian motion to first reach a specified site. The problem has wide applicability in fields as diverse as physics, chemistry, biology, economics, and others [19]. Consider the first-passage of an unstable particle with decay rate  $\lambda$  and diffusion coefficient  $D$  undergoing a random walk from an initial position  $x_0$  to the boundary  $x_b$ . Since there is no further interest in the particle once it has reached  $x_b$ , the particle is considered absorbed at the boundary. One might therefore interpret the residence time as the mean time for a particle to diffuse from the initial location  $x_0 = 0$  to the exit  $x_b = l$  of the detection region. The particle is then absorbed at the exit and cannot return.

Mathematically, it is required to find a probability density function  $p_1(x, t)$  for one-dimensional diffusion of an unstable particle such that  $p_1(x_b, t) = 0$ .

Since the diffusion equation is linear, the sought-for function is readily found from solution (15) by the method of images [20] to be

$$p_1(x, t) = \frac{1}{\sqrt{4\pi Dt}} \left( \exp\left(-\frac{(x-x_0)^2}{4Dt}\right) - \exp\left(-\frac{(x+x_0-2x_b)^2}{4Dt}\right) \right) e^{-\lambda t}. \quad (34)$$

The method of images entails placing an “anti-source” of particles at just such a location as to null the net probability at  $x = x_b$ . From the form of expression (34), one sees that  $p_1(x, t)$  vanishes identically for  $x = x_b$ . **Figure 5** shows plots of pdf (34) as a function of  $x$  for different values of  $t$  with  $x_0 = 0$  and  $x_b = 5$  cm (marked by a vertical dashed line) for the diffusion and decay parameters of  $^{222}\text{Rn}$ . The atom is free to wander over the range  $(-\infty, x_b)$  with vanishing probability at the barrier. The spatial range of physical significance does not extend beyond  $x_b$ .

The probability  $P(x < x_b, t)$  that the particle has not reached the absorbing barrier in time  $t$ , referred to as the survival probability  $S_1(t)$ , is then given by

$$S_1(t) = \int_{-\infty}^{x_b} p_1(x, t) dx = \text{erf}\left(x_b/\sqrt{4Dt}\right) e^{-\lambda t}, \quad (35)$$

which is seen to be of identical form to the cumulative probability (16) of finding the particle in the region  $(\ell \geq x \geq -\ell)$  with *no* absorbing boundaries. Thus, the mean time of first passage to the boundary

$$T_{\text{FP1}} = \int_0^\infty S_1(t) dt = \lambda^{-1} \left( 1 - \exp(-\ell\sqrt{\lambda/D}) \right) \quad (36)$$

is identical under the stated circumstances to the residence time  $T_r$  in (18). Likewise, the probability density function of the random variable whose mean is  $T_{\text{FP1}}$ , which is given by

$$p_{\text{FP1}}(t) = -dS_1(t)/dt, \quad (37)$$

is identical to pdf (33) for  $p_T(t)$ . Although the constrained pdf (34) differs

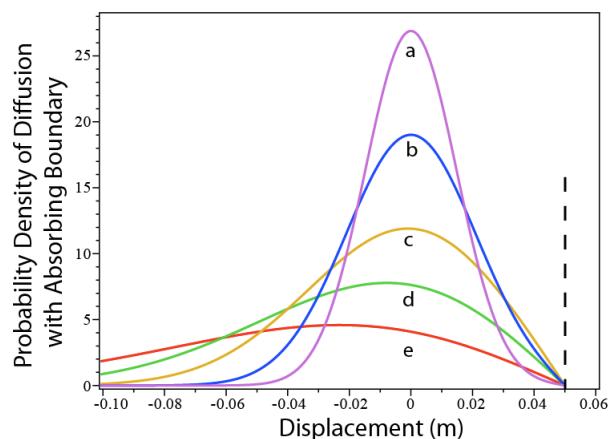


**Figure 5.** Probability density (34) as a function of displacement of Brownian motion with initial location  $x_0 = 0$  and absorbing boundary at  $x_b = 0.05$  m (marked by vertical dashed line) for times (s): (a) 10 (violet); (b) 20 (blue); (c) 50 (gold); (d) 100 (green); (e) 200 (red). Radon parameters are the same as in **Figure 2**.

from the unconstrained pdf (15) mathematically and visually (as seen by comparing **Figure 2** and **Figure 5**), the equivalence of the spatial integrals (16) and (35) follows by making the transformation of variable  $y = x - 2x_b$  in the integral (35), leading to the expression

$$S_1(t) = \frac{e^{-\lambda t}}{\sqrt{4\pi Dt}} \left[ \int_{-\infty}^{x_b} \exp(-x^2/4Dt) dx - \int_{-\infty}^{-x_b} \exp(-y^2/4Dt) dy \right] \tag{38}$$

$$= \frac{e^{-\lambda t}}{\sqrt{4\pi Dt}} \int_{-x_b}^{x_b} \exp(-x^2/4Dt) dx = P(\ell \geq x \geq -\ell, t)$$

identical to probability (16).

A plot of the survival probability  $S_1(t)$  as a function of time is shown in **Figure 6**. Over a short time interval, as shown in the insert,  $S_1(t)$  starts flat and then decreases approximately linearly in time. Over a long time interval,  $S_1(t)$  exhibits a heavy  $t^{-\frac{1}{2}}$  tail due to the asymptotic behavior of the error function.

### 2.4. Comparison of Residence Time with First Passage Time to Two Absorbing Boundaries

From the analyses of the previous two sections one might expect that the residence time of radon within the detection region could also be modeled as the exit time or time of first passage of a particle to either of *two* absorbing boundaries representing the entrance and exit planes of the detection region. This inference would, in fact, be incorrect. It is instructive to understand why this latter system gives rise to a residence time of different functional form and entirely different magnitude.

Mathematically, it is now required to find a probability density function  $p_2(x, t)$  such that a particle diffusing from initial position  $x_0 = 0$  to either boundary  $x_b = \pm\ell$  is absorbed, *i.e.*  $p_2(\ell, t) = p_2(-\ell, t) = 0$ . The solution is

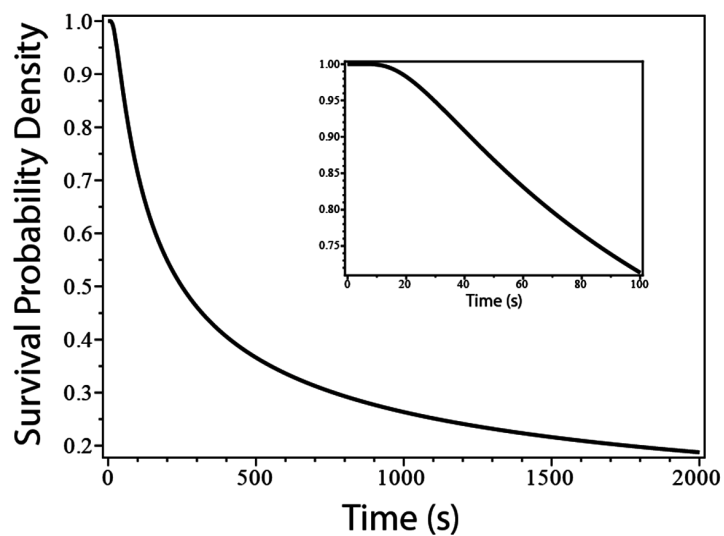


**Figure 6.** Survival probability (35) as a function of time (s) for the absorbing boundary and parameters of **Figure 5**.

again obtained by the method of images, where, in marked contrast to the simple solution (34) for the case of one absorbing boundary, an infinite number ( $N \rightarrow \infty$ ) of image functions placed at  $4n\ell$  and  $(4n-2)\ell$  with  $n = \pm 1, \pm 2, \dots, \pm N$  must be employed to null the probability density at both boundaries. The complete solution takes the form

$$p_2(x, t) = \lim_{N \rightarrow \infty} p_2^{(N)}(x, t, N)$$

$$p_2^{(N)}(x, t, N) = \sum_{n=-N}^N p_2^{(n)}(x, t, n) \quad (39)$$

$$p_2^{(n)}(x, t, n) = \frac{1}{\sqrt{4\pi Dt}} \left( \exp\left(-\frac{(x+4n\ell)^2}{4Dt}\right) - \exp\left(-\frac{(x+(4n-2)\ell)^2}{4Dt}\right) \right) e^{-\lambda t}$$

in which  $p_2^{(n)}(x, t, 0)$  alone enforces only the boundary at  $x = \ell$  as shown in **Figure 5**.

**Figure 7** shows plots of pdf (39), truncated at  $N = 1$ , for  $\ell = 0.05$  m and different values of time  $t \leq 100$  s. Clearly, the particle is confined between the two boundaries, indicated by vertical dashed lines. However, as time increases, the Gaussian functions corresponding to  $n = 0, \pm 1$  spread, and each image function eventually crosses the opposite boundary. To maintain the two boundary conditions, therefore, additional image functions are required. **Figure 8** shows spatial plots of pdf (39) at the fixed time interval  $t = 2000$  s for increasing numbers of image pairs  $N = 4, 5, 6, 7$ . A minimum of 7 image pairs (in addition to the  $n = 0$  Gaussian) is required to maintain absorption of the particle at the two boundaries. As time increases further, additional image pairs must be added. One sees, therefore, why the exact solution for arbitrary time comprises an infinite number of image functions.

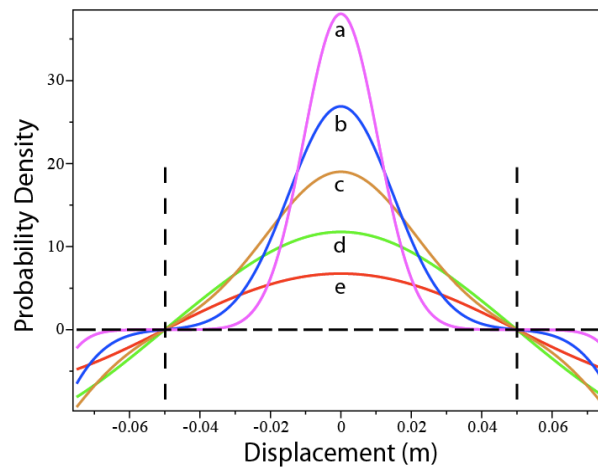


**Figure 7.** Probability density  $p(x, t, N = 1)$  (39) of Brownian motion with two absorbing boundaries at  $\pm\ell = \pm 0.05$  m as a function of distance (m) for times (s): (a) 5 (violet); (b) 10 (blue); (c) 20 (gold); (d) 50 (green); (e) 100 (red). The horizontal dashed black line marks the lower bound 0 of a probability density. Vertical dashed lines mark the boundaries between which the particle is confined.

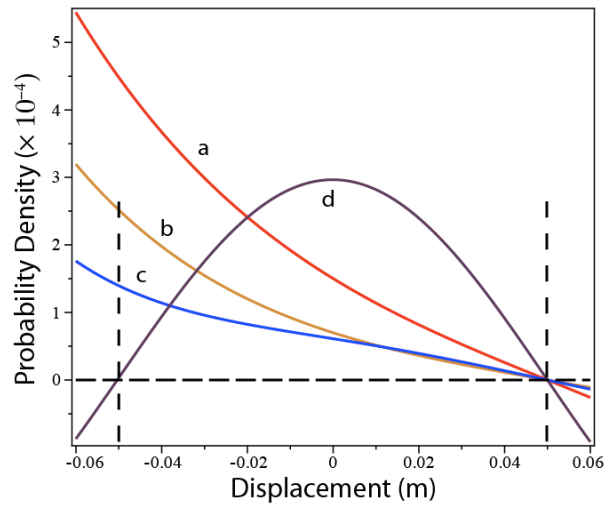


**Figure 8.** Probability density  $p_2^{(N)}(x, t = 2000, N)$  (39) of Brownian motion with two absorbing boundaries at  $\pm \ell = \pm 0.05$  m as a function of displacement (m) for number of image pairs  $N =$  (a) 4 (red); (b) 5 (gold); (c) 6 (blue); (d) 7 (black). The horizontal dashed black line marks the lower bound 0 of a probability density. Vertical dashed lines mark the boundaries between which the particle is confined. For a time interval of 2000 s, a minimum of 7 image pairs is required to confine the particle between the specified boundaries. Plots b, c, d have been scaled up by factors 40, 4000, and 40,000 for visibility.

The survival probability that the particle has not reached either boundary within time  $t$  is given by

$$S_2(t) = \int_{-\ell}^{\ell} p_2(x, t) dx = \sum_{n=-\infty}^{\infty} S_2^{(n)}(t) \tag{40}$$

in which

$$S_2^{(n)}(t) = \int_{-\ell}^{\ell} p_2^{(n)}(x, t, n) dx = \frac{1}{2} \left[ \operatorname{erf} \left( \frac{(4n+1)\ell}{\sqrt{4Dt}} \right) + \operatorname{erf} \left( \frac{(4n-3)\ell}{\sqrt{4Dt}} \right) - 2 \operatorname{erf} \left( \frac{(4n-1)\ell}{\sqrt{4Dt}} \right) \right] e^{-\lambda t} \tag{41}$$

The corresponding first-passage or exit time is

$$T_{\text{FP2}} = \int_0^{\infty} S_2(t) dt = \lim_{N \rightarrow \infty} \sum_{n=-N}^N \left( \int_0^{\infty} S_2^{(n)}(t) dt \right) \tag{42}$$

Performing the integrations and taking the limit in Equation (42) leads to an exit time

$$T_{\text{FP2}} = \frac{1}{\lambda} \left( \frac{(e^{\ell/\zeta} - 1)^2}{(e^{2\ell/\zeta} + 1)} \right), \tag{43}$$

with diffusion length  $\zeta$  given by expression (19). Evaluating relation (43) for the diffusion and decay parameters of  $^{222}\text{Rn}$  with  $\ell = 0.05$  m leads to an exit time  $T_{\text{FP2}} = 113.6$  s, which is very much shorter than the previously obtained residence time (27)  $T_r = 5524.8$  s.

The difference between  $T_{\text{FP2}}$  and  $T_r = T_{\text{FP1}}$  is not just a matter of magnitude, but also of analytical structure. Series expansion of  $T_{\text{FP2}}$  to the first

non-vanishing term in  $\ell/\zeta$  (which is  $\ll 1$  for  $^{222}\text{Rn}$ ) and  $\ell \approx R_\alpha$  leads to

$$T_{\text{FP2}} \approx \ell^2/2D \quad (44)$$

independent of the decay rate  $\lambda$ , in contrast to

$$T_r \approx \ell/\sqrt{D\lambda}. \quad (45)$$

The discrepancy between (44) and (45), which one might have thought described the same physical system—namely, a decaying particle initially at  $x = 0$  in Brownian motion between two locations at  $x = \pm\ell$ —arises because the two physical systems are not at all equivalent.

When a randomly moving particle reaches one or the other of the two absorbing boundaries it is removed from the system. This is *not* the case for radon diffusing through a region of width  $2\ell$  overlying the detector. The particle in this system can exit the region of detectability or diffuse back into it with a probability of 50%. The space open to the radon atom is effectively infinite ( $-\infty < x < \infty$ ), whereas the space open to the particle between two absorbing barriers is finite ( $-\ell < x < \ell$ ). In the system with one absorbing barrier at  $x = \ell$ , whose time of first passage  $T_{\text{FP1}}$  is equal to the residence time  $T_r$ , the region of space available to the particle ( $-\infty < x < \ell$ ) is still infinite.

To understand the physical significance of the time interval (44) in the context of radon diffusion in an open volume (no boundaries) consider the temporal value at which pdf (33) for the residence time  $T_r$  is maximum. Since the statistical lifetime  $\lambda^{-1}$  is very long ( $\lambda^{-1} \sim 5.5$  d) compared with the mean residence time ( $T_r \sim 1.5$  h), one can, for the purposes of finding the maximum, set  $\lambda$  equal to 0, *i.e.* drop the second term on the right side of the second equality in (33). The location of the peak of the first term (*i.e.* Smirnov density  $\propto t^{-3/2}$ ) is then obtained by setting the time derivative of its logarithm to zero, and leads to

$$t_{\text{max}} = \ell^2/6D, \quad (46)$$

which, to within a numerical factor, has the same form as  $T_{\text{FP2}}$ . Evaluated for radon diffusivity  $D_0$  and length  $\ell = 0.05$  m, one obtains  $t_{\text{max}} \sim 38$  s, in close agreement with the maximum of the plot in **Figure 4**.

It is worth noting here, although the derivation is given elsewhere [21], that the mean exit time (referred to as time to capture)  $T_C(x)$  of a stable particle diffusing from some initial position  $x_0$  to either of two absorbing boundaries can be calculated directly from solution of a Poisson equation

$$D\nabla^2 T_C(x_0) + 1 = 0 \quad (47)$$

with implementation of appropriate boundary conditions. For a stable particle undergoing a one-dimensional random walk between absorbing boundaries at  $-\ell$  and  $+\ell$  the solution to (47) is

$$T_C(x_0) = (\ell^2 - x_0^2)/2D, \quad (48)$$

which reduces to  $\ell^2/2D$  for the chosen initial condition  $x_0 = 0$ . As expected for consistency, this is also the result obtained by taking the limit of  $T_{\text{FP2}}$  in re-

lation (43) as  $\lambda$  approaches 0

$$\lim_{\lambda \rightarrow 0} (T_{FP2}) = \ell^2 / 2D. \tag{49}$$

In the case of an unstable particle with decay rate  $\lambda$  diffusing between two absorbing boundaries, it can be shown [22] that the corresponding time to capture follows from an equation of the form

$$D\nabla^2 T_C(x_0) - \lambda T_C(x_0) + 1 = 0 \tag{50}$$

and leads to a solution that for  $x_0 = 0$  reduces exactly to  $T_{FP2}$  in relation (43).

### 3. Mutual Consistency of Brownian Motion and Mass Diffusion

The preceding sections have demonstrated the equivalence of residence times calculated from models of a) free diffusion of a macroscopic sample of radon gas under a concentration gradient, and b) unconstrained Brownian motion of individual radon atoms moving forward or backward independently with equal probability—*i.e.* oblivious to the concentration gradient. Since approach a) appears to involve directed motion attributable to a kind of force (*i.e.* gradient of a potential<sup>1</sup>) and approach b) clearly involves random motion in the absence of any force, it may not be immediately apparent why the two approaches actually describe the same physical process. Here, in brief, is an explanation, as illustrated schematically in **Figure 9**. Suppose there are  $N(x)$  particles at  $x$  and

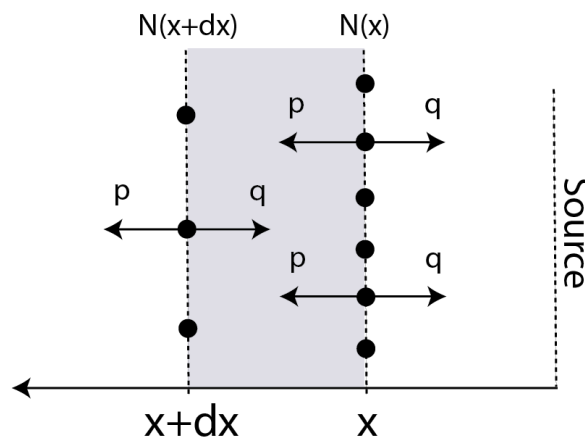


**Figure 9.** Relation of Brownian motion to Fick’s law. Individual atoms (black dots) undergo a random walk to the left with probability  $p$  or to the right with probability  $q$ . For an unbiased walk,  $p = q = 0.5$ . Since the number of atoms  $N(x) > N(x + dx)$ , more atoms move to the left at  $x$  than atoms move to the right at  $x + dx$ . The net flux to the left through  $dx$  is proportional to the gradient  $-dN/dx$  even though individual atoms are insensitive to the gradient.

<sup>1</sup>From a thermodynamic perspective, the potential responsible for diffusion is the chemical potential  $\mu$ , which, for an ideal gas, is given by  $\mu = \mu_0 + k\theta \ln(n)$ , where  $k$  is Boltzmann’s constant,  $\theta$  is the absolute temperature,  $n$  is the particle density, and  $\mu_0$  is the chemical potential of some established reference state.

$N(x + dx)$  particles at  $x + dx$ , and that each particle has a probability  $p$  to move left and  $q$  to move right along the  $x$ -axis with equal speed. The net transport (or differential flux) of particles to the left through the region  $dx$  is given to first order in  $dx$  by

$$j_D(x) + j_F(x) dx \propto pN(x) - qN(x + dx) = (p - q)N(x) - q \frac{\partial N}{\partial x} dx. \quad (51)$$

For equal probabilities  $p = q = 1/2$ , the drift current density  $j_D(x)$  vanishes, and relation (51) leads to a fluctuation current density

$$j_F(x) \propto -\frac{1}{2} \frac{dN(x)}{dx} \quad (52)$$

that captures the physical content of Fick's law. The greater transport of particles to the left does not arise because there is an asymmetric force acting on individual particles, but because of the greater number of particles to enter the region  $dx$  from the right (closer to the source) than from the left. For each particle, however, the two directions of motion are equally probable. The applicability of Fick's law to radon diffusion has, in fact, been tested and confirmed experimentally [23].

#### 4. Conclusions

Implementation of the newly introduced procedure [4] to measure indoor radon activity concentration quantitatively and accurately by means of two GM detectors requires knowledge of the rate at which radon atoms pass through the open detection region, or, equivalently, the mean time spent by a radon atom within the detection region.

The analyses in this paper have established that one must exercise caution in adopting a stochastic model to describe the time spent by a radioactive atom in the detection region. For example, although it may seem reasonable to define (and presumably measure) the residence time as the mean time for an atom within the detection region to first reach either the entrance or exit plane, this choice is physically unsatisfactory. It ignores the possibility that the atom, having reached a boundary, can proceed away from or back into the detection region with equal probability. As a consequence, this first-passage or exit time, given approximately by

$$T_{FP2} \sim \frac{(\text{length of detection region})^2}{(\text{diffusion coefficient})}, \quad (53)$$

is too short and would lead to a measurement of radon concentration that is significantly lower than actual (see Equation (27) of Ref. [4]). On the other hand, the present analysis has established the equivalence of defining the residence time as *either* a) the mean time spent by the atom between the entrance and exit planes of the detection region irrespective of how often the atom may pass through a boundary *or* b) the time the atom first reaches the exit plane of the detection region. The two times are identical mathematically and given ap-

proximately by

$$T_r = T_{\text{FP1}} \sim \frac{(\text{length of detection region})}{\sqrt{(\text{diffusion coefficient})(\text{radioactive decay rate})}}. \quad (54)$$

Given the system parameters  $D$ ,  $\lambda$ ,  $\ell$  (diffusion coefficient, decay rate, half-length of detection region) of the diffusion of a radioactive atom, expressions (53) and (54) comprise the only two independent combinations that lead to quantities with the dimension of time. The statistical or geometric interpretation of these times can be inferred from the probability density function (33) plotted in **Figure 4**. This pdf exhibits a sharp rise to a maximum  $T_{\text{max}}$  and then an infinitely long, heavy tail. Time interval (53) is a measure of  $T_{\text{max}}$ , whereas interval (54) is a measure of the first moment  $T_r$ , which constitutes the physical residence time. The figure illustrates why  $T_r \gg T_{\text{max}}$ . The finiteness of  $T_r$  is due to the transient existence of the radioactive sample. For a stable particle,  $\lambda = 0$  and the first moment of the resulting Smirnov density ( $\propto t^{-3/2}$ ) is infinite, indicative of the possibility for a stable particle to undertake an infinitely long random walk. By contrast, approximately half of a sample of radioactive particles have decayed within a time  $\lambda^{-1} \ln 2$ , which for  $^{222}\text{Rn}$  is  $\sim 3.8$  days.

## References

- [1] Andersson, K.G. (2009) Airborne Radioactive Contamination in Inhabited Areas. Elsevier, Amsterdam, 1-20.
- [2] Zeeb, H. and Shannoun, F., Eds. (2009) WHO Handbook on Indoor Radon: A Public Health Perspective, Summary Statistics at [http://www.who.int/phe/radiation/background\\_radon/en/](http://www.who.int/phe/radiation/background_radon/en/)
- [3] A Citizen's Guide to Radon (2012) US Environmental Protection Agency EPA-402/K-12/002. <http://www.epa.gov/radon>
- [4] Silverman, M.P. (2016) Method to Measure Indoor Radon Concentration in an Open Volume with Geiger-Mueller Counters: Analysis from First Principles. *World Journal of Nuclear Science and Technology*, **6**, 232-260. <https://doi.org/10.4236/wjnst.2016.64024>
- [5] Lapp, R.E. and Andrews, H.L. (1972) Nuclear Radiation Physics. 4th Edition, Prentice-Hall, Englewood Cliffs, NJ, 198-200.
- [6] Annunziata, M.F. (1998) Handbook of Radioactivity Analysis. Academic Press, New York, 6-8.
- [7] Tsoulfanidis, N. and Landsberger, S. (1995) Measurement & Detection of Radiation. 2nd Edition, Taylor & Francis, Washington DC, 106.
- [8] Hull, D.E. (1958) The Total-Count Technique: A New Principle in Flow Measurement. *International Journal of Applied Radiation and Isotopes*, **4**, 1-15. [https://doi.org/10.1016/0020-708X\(58\)90020-6](https://doi.org/10.1016/0020-708X(58)90020-6)
- [9] Reeve, D.R. and Crozier, A. (1977) Radioactivity Monitor for High-Performance Liquid Chromatography. *Journal of Chromatography*, **137**, 271-282. [https://doi.org/10.1016/S0021-9673\(00\)81350-3](https://doi.org/10.1016/S0021-9673(00)81350-3)
- [10] Nazaroff, W.W. and Nero Jr., A.V. (Eds.) (1988) Radon and Its Decay Products in Indoor Air. Wiley, New York, 65-69.
- [11] Environmental Science Division, Argonne National Laboratory. Effective Radon

Diffusion Coefficient. <http://web.ead.anl.gov/resrad/datacoll/radon.htm>

- [12] Bellotti, E., Broggini, C., Di Carlo, G., Laubenstein, M. and Menegazzo, R. (2015) Precise Measurement of the  $^{223}\text{Rn}$  Half-Life: A Probe to Monitor the Stability of Radioactivity. *Physics Letters B*, **743**, 526-530.
- [13] Wallace, P.R. (1984) *Mathematical Analysis of Physical Problems*. Dover, New York, 355-383.
- [14] Lea, S.M. (2004) *Mathematics for Physicists*. Brooks/Cole, Belmont, 354.
- [15] Feller, W. (1957) *An Introduction to Probability Theory and Its Applications*. Vol. 1, Wiley, New York, 304-305, 368-370.
- [16] Franklin, P. (1964) *A Treatise on Advanced Calculus*. Dover, New York, 347-349.
- [17] Hughes, B.D. (1995) *Random Walks and Random Environments*. Vol. 1, Random Walks. Oxford University Press, Oxford, 205-206.
- [18] Krapivsky, P., Redner, S. and Ben-Naim, E. (2010) *A Kinetic View of Statistical Physics*. Cambridge University Press, Cambridge, 32-35.  
<https://doi.org/10.1017/CBO9780511780516>
- [19] Redner, S. (2007) *A Guide to First Passage Processes*. Cambridge University Press, Cambridge.
- [20] Carslaw, H. and Jaeger, J. (1959) *Conduction of Heat in Solids*. 2nd Edition, Oxford University Press, Oxford, 273-281.
- [21] Berg, H.C. (1993) *Random Walks in Biology*. Princeton University Press, Princeton, 42-47.
- [22] Silverman, M.P. (2017) Unpublished Work in Preparation for Publication.
- [23] Sasaki, T., Gunji, Y. and Iida, T. (2007) Transient-Diffusion Measurements of Radon: Fick's Law Confirmation and  $^{218}\text{Po}/^{214}\text{Po}$  Behavior Determination. *Journal of Nuclear Science and Technology*, **44**, 1330-1336.  
<https://doi.org/10.1080/18811248.2007.9711379>
- [24] Goody, R. and Walker, J. (1972) *Atmospheres*. Prentice-Hall, Englewood Cliffs, 4-11.
- [25] Tabor, D. (1979) *Gases, Liquids, and Solids*. 2nd Edition, Cambridge University Press, Cambridge, 43-51.
- [26] Vardavas, I. and Taylor, F. (2011) *Radiation and Climate: Atmospheric Energy Budget from Satellite Remote Sensing*. Oxford University Press, Oxford, 42-48.

## Appendix 1:

### Density Profile of Radon Gas in a Uniform Gravitational Field

The point at issue is whether the vertical density profile of radon gas is affected by gravity over a dimension of order of the alpha-particle range  $R_\alpha \sim 5 \text{ cm}$ . If that were the case, then analysis of the residence time of a radon atom in the detection volume would require use of an anisotropic Green's function.

The barometric law for equilibrium gas pressure  $P(z)$  as a function of altitude  $z$  is [24]

$$dP(z)/dz = -mgn(z) \quad (55)$$

where  $n(z)$  is the number density (particles per volume),  $m$  is the mass per particle, and  $g$  is the acceleration of gravity taken here to be a constant  $9.8 \text{ m}\cdot\text{s}^{-2}$  close to the Earth's surface. The gas is assumed to behave ideally with equation of state [25]

$$P = nk\theta \quad (56)$$

where  $\theta$  is the absolute temperature in Kelvin (K) and  $k = 1.38 \times 10^{-23} \text{ J/K}$  is Boltzmann's constant. The two cases of potential relevance to the measurement of indoor radon are the isothermal and adiabatic atmospheres.

(A) Isothermal Atmosphere (Constant Temperature  $\theta$ )

Elimination of pressure by substitution of Equation (56) into (55) leads to a logarithmic differential equation for density whose solution is

$$n(z)/n(0) = \exp(-z/\xi) \quad (57)$$

with scale parameter

$$\xi \equiv k\theta/mg = N_A k\theta/Mg. \quad (58)$$

In the second equality of (58)  $M$  is the radon molar mass and  $N_A \sim 6.02 \times 10^{23}$  is Avogadro's number.

For  $^{222}\text{Rn}$  ( $M = 0.222 \text{ kg}$ ) at room temperature ( $\theta \sim 300 \text{ K}$ ), the scale parameter is approximately  $\xi_0 \approx 1146 \text{ m}$ , and the ratio  $R_\alpha/\xi_0 \approx 3.5 \times 10^{-5} \ll 1$ . Therefore the density profile (57) over the detection volume is essentially constant  $n(z)/n(0) \approx 1 - z/\xi_0 \approx 1$  for  $z$  in the range ( $R_\alpha \geq z \geq 0$ ).

(B) Adiabatic Atmosphere (Constant Entropy)

Although a room (e.g. a laboratory) or a building may be kept under isothermal conditions, the lowest section of the Earth's atmosphere (the troposphere) is not isothermal, but more accurately described by the adiabatic constitutive relation [26]

$$P(z)/P(0) = (n(z)/n(0))^\gamma, \quad (59)$$

where  $\gamma$  is the ratio of heat capacity at constant pressure to the heat capacity at constant volume. For an atmosphere comprised predominantly of diatomic molecules, one has  $\gamma = 7/5 = 1.4$ . Use of relation (59) together with (55) and (56) leads to the atomic density

$$n(z)/n(0) = \left(1 - (1 - \gamma^{-1})(z/\xi(0))\right)^{\frac{1}{\gamma-1}} \quad (60)$$

with the scale parameter  $\xi(0)$  defined by Equation (58) in terms of the ground-level temperature  $\theta_0$ . Since it is evident from part (A) that the second term in the bracketed expression of (60) is  $\ll 1$ , one can expand the bracket in a Taylor series to first order to obtain  $n(z)/n(0) \approx 1 - z/\gamma\xi_0$  for the parameters (room temperature and radon molar mass) used in part (A). Since  $\gamma > 1$ , the density profile of the radon gas is even more uniform in the adiabatic atmosphere than in the isothermal atmosphere.

It is to be concluded, therefore, that gravity has a negligible effect on the equilibrium density profile of radon within the detection volume, and that use of the isotropic Green's function for calculating the radon residence time is justified.

## Appendix 2:

### Use of the Cumulative Distribution Function to Calculate Expectation Values

If  $f(x)$  is the probability density function (pdf) of a random variable  $X$ , and  $F(x) = \int_{-\infty}^x f(x') dx'$  is the corresponding cumulative distribution function (cdf), then the expectation value  $\langle X \rangle$  is given by

$$\begin{aligned} \langle X \rangle &= \int_{-\infty}^{\infty} xf(x) dx = \int_{-\infty}^{\infty} x dF(x) \\ &= \int_{-\infty}^0 x dF(x) + \int_0^{\infty} x dF(x). \end{aligned} \quad (61)$$

Integration by parts of the two integrals on the second line of (61) yields

$$\begin{aligned} \int_{-\infty}^0 x dF(x) &= -\int_{-\infty}^0 F(x) dx \\ \int_0^{\infty} x dF(x) &= -\int_0^{\infty} x d(1-F(x)) = \int_0^{\infty} (1-F(x)) dx \end{aligned} \quad (62)$$

where use was made of the properties  $F(-\infty) = 0$ ,  $F(\infty) = 1$ ,  $[xF(x)]_{x=0} = 0$ ,  $[xF(x)]_{x=-\infty} = 0$ .

It then follows from (61) that

$$\langle X \rangle = \int_0^{\infty} (1-F(x)) dx - \int_{-\infty}^0 F(x) dx. \quad (63)$$

For an intrinsically positive variable  $X$  the second term on the right side of (63) vanishes. In that case, the same procedure can be used to show that the variance of  $X$  is given by

$$\text{var}(X) = 2 \int_0^{\infty} x(1-F(x)) dx - \left( \int_0^{\infty} (1-F(x)) dx \right)^2. \quad (64)$$